

Alternative approaches to staggered PRT clutter filtering

GREGORY MEYMARIS*

National Center for Atmospheric Research, Boulder, Colorado

JOHN C. HUBBERT

National Center for Atmospheric Research, Boulder, Colorado

MICHAEL DIXON

National Center for Atmospheric Research, Boulder, Colorado

1. Introduction

Staggered PRT (pulse repetition) is a popular technique to mitigate the range-velocity dilemma of weather radars. The unambiguous range is based on the longer PRT while the largest time interval that divides evenly the two PRTs gives the unambiguous velocity (Zrnić and Mahapatra 1985). The major limitation of the staggered PRT technique has been clutter filtering. Since the time-series for a resolution volume is not equi-spaced, traditional filtering techniques such as time domain IIR (infinite impulse response) filtering or spectral domain filtering (based on the Discrete Fourier Transform (DFT)) are not immediately applicable. Recently Sachidananda and Zrnić (2000; 2002) introduced a staggered PRT clutter filtering algorithm based on the interpolation of the time-series to equi-spaced samples. This is done by interleaving zeros into the time-series to create equi-spaced time-series. The interpolated time-series is then transformed with a DFT. The resulting spectrum contains 5 replicas of the intrinsic underlying spectrum. Fairly complicated matrix mathematics is used to filter the spectra and estimate the power, mean velocity, and spectrum width.

In this paper we discuss a novel technique in which the time-series is separated into two equi-spaced time-series and then a spectral notch clutter filter can be employed. The two filtered sequences are then recombined to once again create a staggered PRT sequence. The velocity and power can then be calculated in standard fashion. Another similar technique based on regression filtering (Torres

and Zrnić 1999) is also proposed.

2. Alternative SPRT Clutter Filtering Techniques

A typical staggered PRT sequence is shown in Fig. 1. Sequence (A) is the staggered PRT sequence with the two staggers periods T_1 and T_2 ; in this paper, the $2/3$ stagger is assumed, which means that $T_1 = 2T_2/3$. Denote the time-series samples s_1, s_2, \dots, s_M (where M is the total number of samples). Two sequences are created by taking alternate samples and separating them as indicated by the red and blue lines and the even and odd samples. The resulting two sequences have a period of $T_1 + T_2$. These equi-spaced sequences can then be filtered in the time domain or the frequency domain. If they are filtered in the frequency domain, the sequences are subsequently transformed using an inverse DFT. The resulting time-series are then interleaved to produce the filtered staggered PRT sequence corresponding to Fig. 1A.

It is instructive to compare the Sachidananda and Zrnić (2002) technique (SACHI) and the simplified staggered PRT technique (SSPRT) via a numerical example. Let $T_1 = 785 \mu\text{s}$ and $T_2 = 1177 \mu\text{s}$ so that $T_1 + T_2 = 1962 \mu\text{s}$. The SACHI zero-interpolated sequence has a period $T_u = 393 \mu\text{s}$. Therefore, the unambiguous velocity for SACHI is 67 m s^{-1} while the unambiguous velocity for SSPRT sequence, based on period of $1962 \mu\text{s}$, is 13 ms^{-1} . The SACHI technique creates 5 “replicas” (phase

* *Corresponding author address:*

Gregory Meymaris, RAL, NCAR
1850 Table Mesa Dr., Boulder, CO 80305
E-mail: meymaris at ucar.edu

and amplitude modulated) of the true clutter signal spectrum equi-spaced over the entire unambiguous velocity range of 134 ms^{-1} . Thus the spectrum replicas are separated 27 ms^{-1} intervals. The performance of the SACHI clutter filter degrades when there is weather located at these 27 ms^{-1} intervals (i.e., weather can be eliminated by the clutter filter causing biased velocity and reflectivity estimates). For SSPRT, if weather signal is located close to 0 ms^{-1} , this weather signal can also be attenuated causing biased estimates. Since the unambiguous velocity is 13 ms^{-1} , weather with $27k \text{ ms}^{-1}$, where k is an integer, will “wrap back” to 0 ms^{-1} and thus these weather signals can also be attenuated by the clutter filter. Therefore, both SACHI and SSPRT can suffer performance degradation when weather has velocity close to $27k \text{ ms}^{-1}$ (depending on the width of the clutter filter).

Figures 2-5 show various spectral representations for a simulated weather and overlaid clutter case. The original spectra sampled at $393 \mu\text{s}$ with 160 samples is shown in figure 2. This can be thought of as the spectrum that the staggered PRT techniques are trying to recover. In figure 3, the spectra from the SACHI technique is shown (i.e. the original time-series is down-sampled using SPRT, the missing values are then “interpolated” back in with 0’s, and then the spectrum is calculated). With the SSPRT technique, the SPRT time-series was separated into even and odd time-series, and the spectra are calculated. The resulting spectra are shown in figure 4, zoomed into the 13 ms^{-1} Nyquist interval, and in figure 5, shown on the extended Nyquist interval like figures 2 and 3.

3. Algorithms

a. SSPRT

The SSPRT method works as follows. The time-series is separated into even and odd time-series (each with PRT $T_1 + T_2$). The time-series are windowed using von Hann window function, and the FFT is computed. To filter the clutter, we used Gaussian Model Adaptive Processing (GMAP) clutter filter (Siggia and R. Passarelli 2004). If GMAP determines that clutter exists, then GMAP not only attempts to remove the clutter power, it also attempts to reconstruct the weather by assuming a Gaussian shape. However, care must be taken for staggered PRT data because it is necessary to also reconstruct the phases as well. Or more precisely the difference between the phases of the two complex

spectra, since this contains important information. Before GMAP is applied, using the phase angle between the complex spectra at a spectral bin as well as the velocity value at that bin, a determination can be made as to which of the 5 intervals the data in that bin likely came from. There is some noise in the estimate so a de-speckle type filter is applied to fix isolated misclassifications. Continuing the simulated clutter and weather case above, figure 6 shows the interval determination for the spectra in figure 4. In theory, the spectrum can then be de-aliased, which is shown in figure 7. GMAP could then be applied and the moments could then be calculated.

Alternatively, GMAP can be applied to each spectrum (even and odd), and then the interval determination (made before applying GMAP) can be used to assign the phases between the complex spectra for the bins that GMAP modified. An inverse FFT is then applied to each spectrum, and the time-series are “zippered” back together. The power, mean velocity and spectrum width can then be calculated using the standard techniques (Zrnić and Mahapatra 1985; Sachidananda et al. 1999; Torres et al. 2004).

b. Regression Filter

Another approach which has some significant promise is to use a regression filter as described by Torres and Zrnić (1999), instead of GMAP. Because the regression filter is a time-domain filter, a few details change. A least-squares polynomial fit is subtracted from the time-series data (real and imaginary parts are treated separately). This is a time-domain high-pass filter. Spectral reconstruction can then be performed. To do this the time-series can again be split into even and odd time-series and the spectra calculated for each. An advantage of the regression filter is that it effectively removes, or at least reduces, the need to use a window function when calculating the spectra. For the spectral reconstruction, the 3 or 5 points centered at 0 velocity can be linearly interpolated over. Something more complex like what is done in GMAP could also be done. The phases and then finally spectral moments are computed as in SSPRT.

The even and odd spectra from the same example after the regression filter (order 5 polynomial) has been applied is shown in figure 8. This is analogous to 4 except that the filter has already been applied. The interval determination is shown in figure b, and the de-aliased spectrum is shown in figure 9. Again, the moments could then be calculated on this de-aliased spectrum.

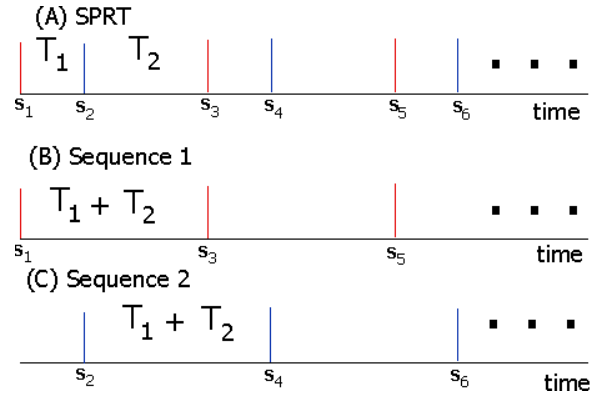


Figure 1: (A) A staggered PRT sequence. (B) and (C) show two equi-spaced sequences consisting of the even and odd samples of (A).

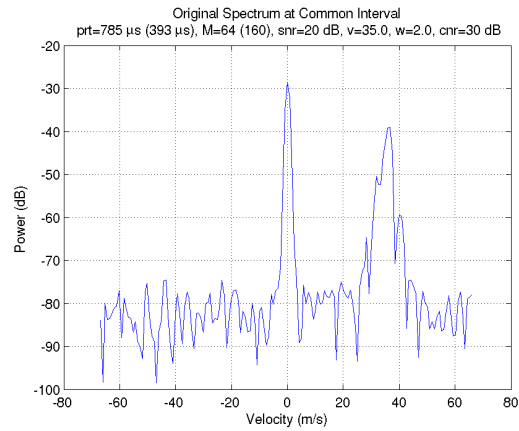


Figure 2: Spectrum of a simulated weather and clutter echo. The simulation parameters are $\lambda = 10.5$ cm, PRT of 393 μ s, 160 samples, 20 dB SNR.

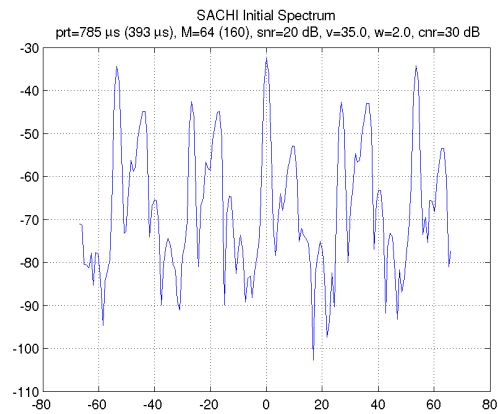


Figure 3: SACHI Spectrum of a simulated weather and clutter echo. The simulation parameters are $\lambda = 10.5$ cm, $T_1 = 785$ μ s, 64 staggered PRT samples, 20 dB SNR.

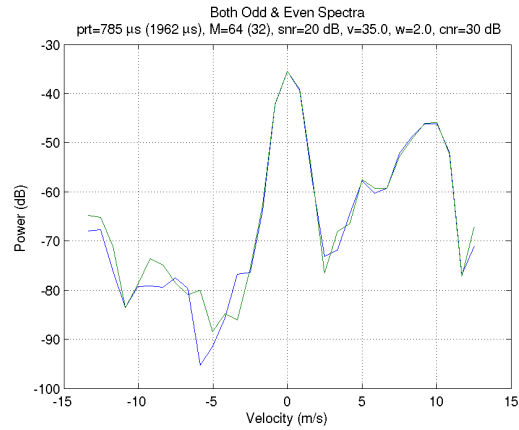


Figure 4: SSPRT Spectra (even and odd) of a simulated weather and clutter echo. The simulation parameters are $\lambda = 10.5$ cm, $T_1 = 785$ μ s, 64 staggered PRT samples, 20 dB SNR.

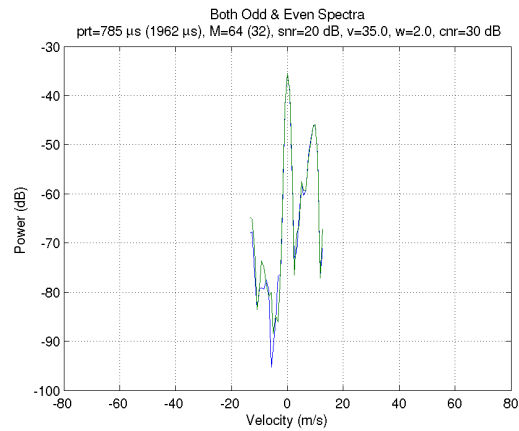


Figure 5: SSPRT Spectra (even and odd) of a simulated weather and clutter echo on the extended Nyquist interval. The simulation parameters are $\lambda = 10.5$ cm, $T_1 = 785$ μ s, 64 staggered PRT samples, 20 dB SNR.

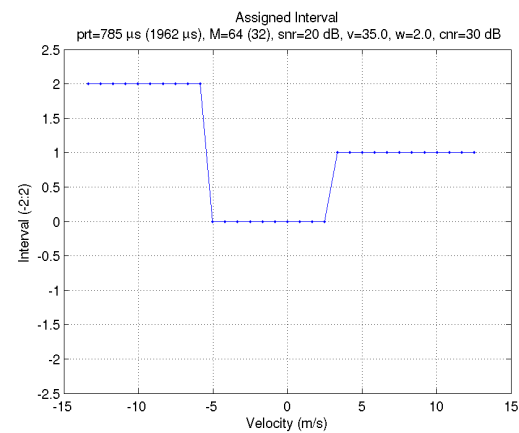


Figure 6: SSPRT interval determination of a simulated weather and clutter echo shown in figure 4. The simulation parameters are $\lambda = 10.5$ cm, $T_1 = 785$ μ s, 64 staggered PRT samples, 20 dB SNR.

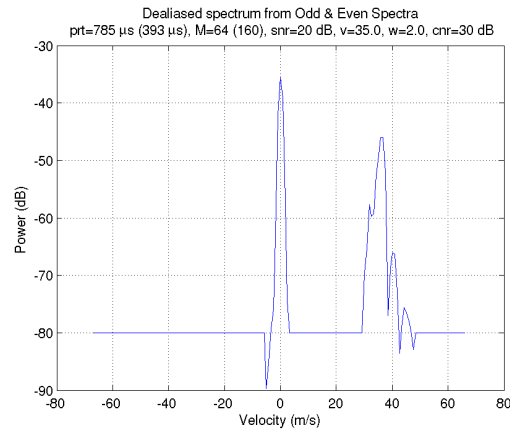


Figure 7: SSPRT de-aliased spectrum of a simulated weather and clutter echo shown in figure 4. The simulation parameters are $\lambda = 10.5$ cm, $T_1 = 785$ μ s, 64 staggered PRT samples, 20 dB SNR.

Alternatively, the interval determination can be used to assign the phases between the complex spectra for the bins that the regression filter modified. An inverse FFT is then applied to each spectrum, and the time-series are “zippered” back together. The power, mean velocity and spectrum width can then be calculated using the standard techniques

4. Conclusions

The SSPRT and regression filtering techniques are promising clutter filtering techniques in at least some scenarios. It has the advantage that it is quite simple to understand, building from more standard techniques than does SACHI. A detailed study of the scenarios in which these techniques are better than SACHI, and vice versa, needs to be performed.

5. Acknowledgment

This research was supported in part by the ROC (Radar Operations Center) of Norman OK. Any opinions, findings and conclusions or recommendations expressed in this publication are those of the author(s) and do not necessarily reflect the views of the ROC.

References

Sachidananda, M. and D. Zrnić, 2000: Clutter Filtering and Spectral Moment Estimation for Doppler

Weather Radars Using Staggered Pulse Repetition Time (PRT). *Journal of Atmospheric and Oceanic Technology*, **17**, 323–331.

Sachidananda, M. and D. Zrnić, 2002: An Improved Clutter Filtering and Spectral Moment Estimation Algorithm for Staggered PRT Sequences. *Journal of Atmospheric and Oceanic Technology*, **19**, 2009–2019.

Sachidananda, M., D. S. Zrnić, and R. J. Doviak, 1999: Signal design and processing techniques for WSR-88D ambiguity resolution. part-3. Technical report, National Severe Storms Laboratory.

Siggia, A. and J. R. Passarelli: 2004, Gaussian model adaptive processing (gmap) for improved ground clutter cancellation and moment calculation. *Proceedings of Third European Conference on Radar in Meteorology and Hydrology*, ERAD, Visby, Gotland, Sweden, 67–73.

Torres, S., M. Sachidananda, and D. S. Zrnić, 2004: Signal design and processing techniques for WSR-88D ambiguity resolution: Phase coding and staggered PRT data collection, implementation, and clutter filtering. part-8. Technical report, National Severe Storms Laboratory.

Torres, S. and D. S. Zrnić, 1999: Ground clutter canceling with a regression filter. *J. Atmos. Oceanic Technol.*, **16**, 1364–1372.

Zrnić, D. S. and P. Mahapatra, 1985: Two Methods of Ambiguity Resolution in Pulse Doppler Weather Radars. *Aerospace and Electronic Systems, IEEE Transactions on*, **AES-21**, 470–483.

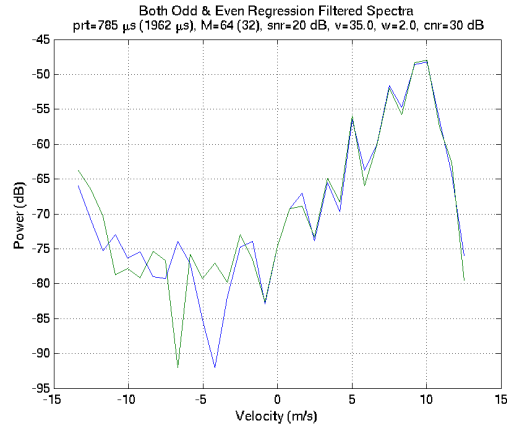
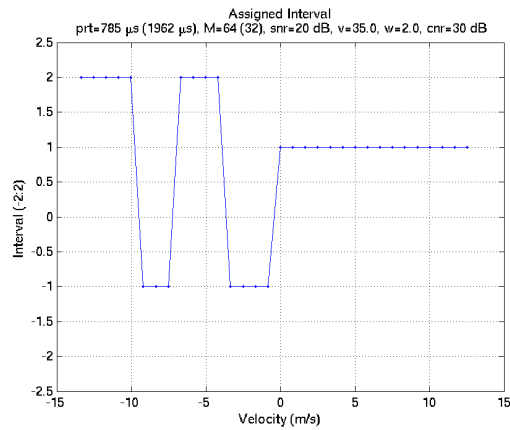


Figure 8: SSPRT Regression Spectra (even and odd), with no window used, of a simulated weather and clutter echo. The simulation parameters are $\lambda = 10.5$ cm, $T_1 = 785 \mu\text{s}$, 64 staggered PRT samples, 20 dB SNR. The polynomial order used was 5.



SSPRT Regression interval determination of a simulated weather and clutter echo. The simulation parameters are $\lambda = 10.5$ cm, $T_1 = 785 \mu\text{s}$, 64 staggered PRT samples, 20 dB SNR. The polynomial order used was 5.

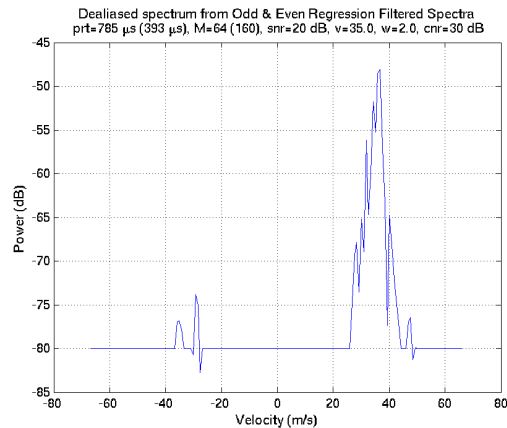


Figure 9: SSPRT de-aliased regression Spectra (even and odd), with no window used, of a simulated weather and clutter echo. The simulation parameters are $\lambda = 10.5$ cm, $T_1 = 785 \mu\text{s}$, 64 staggered PRT samples, 20 dB SNR. The polynomial order used was 5.